Predicted of grinding forces in ultrasonic vibration grinding of fused silica glass based on the stochastic distributed abrasive grits

Cheng Huang[1,2,3,#], Yupeng Xiong[1,2,3], Chunyang Du[1,2,3], Tao Lai[1,2,3], Shanyong Chen[1,2,3], Xiaoqiang Peng[1,2,3] and Ming Zhou[4]

1 Laboratory of Science and Technology on Integrated Logistics Support, College of Intelligence Science and Technology, National University of Defense Technology, Changsha, Hunan 410073, P.R of China
2. Hunan Key Laboratory of Ultra-Precision Machining Technology, College of Intelligence Science and Technology, National University of Defense Technology, Changsha 410073, China
3. Nanhu Laser Laboratory, National University of Defense Technology, Changsha 410073, China
4 School of Mechatronic Engineering, Harbin Institute of Technology, Harbin, Heilongjiang 150001, P.R of China
Corresponding Author / Email: hithuangcheng@163.com, TEL: +86-13187089709

KEYWORDS: Ultrasonic vibration grinding, Grinding force, Fused silica glass, Stochastic grits

Ultrasonic vibration grinding (UVG) has been recognized as an efficient machining method for hard and brittle materials. In this paper, a theoretical model was proposed for predicting grinding force in UVG of fused silica glass with consideration of the stochastic distributed abrasive grits. Since the protrusion height of diamond grits was closely related to the grinding force, the modelling of the wheel end-face morphologies was performed to obtain the protrusion height data of diamond grits. Based on indention theory combined with energy perspective, a material removal rate model was proposed for establishing the grinding force model. Experiments were conducted to verify the validity of the proposed model, and the mean error between predicted and experimental force is 4.87%. The proposed model could be used in selecting process parameters for realizing high efficiency and precision UVG machining of fused silica glass.

1. Introduction

Fused silica glass has superior properties such as high linear transmission, wide transmission range, high mechanical strength, and low thermal expansion coefficient[1]. It covers a broad range of applications in related industries in recent years, especially in high-power laser systems[2]. All these advanced components demand high precision and low damages in manufacturing processes. However, conventional machining methods for fused silica glass easily induce surface/subsurface damage due to its high hardness, brittleness, and low fracture toughness which affects the component performances[3]. Therefore, it is challenging to achieve the desired accuracy, high efficiency, and cost-effective processing for Fused silica glass.

Ultrasonic vibration grinding (UVG) is a novel hybrid machining technology with multiple benefits in terms of reducing grinding force, tools wear, and increasing material removal rate[4]. It combines the material removal mechanism of conventional grinding process and ultrasonic machining[5]. A special designed hollow-cone diamond wheel is utilized in the process. The diamond grinding wheel vibrates along the axial direction at an amplitude of about 1-10μm and a frequency of about 15-40kHz while it rotates and fed toward the workpiece. UVG has been recognized as an efficient machining method for hard and brittle materials, including fused silica glass, sapphire, and ceramics[6]. To some extent, the problems in fused silica glass manufacturing are resolved by the introduction of ultrasonic machining technology to conventional grinding process. Nowadays perpetual efforts are being made by researchers to explore the full potential of the UVG method for the benefits of suppression manufacturing defects and enhanced machining efficiency.

The magnitude of grinding force is an important output variable during grinding process which affects directly the machined surface/subsurface quality and machining precision of hard and brittle materials[7, 8]. Research on theoretical prediction of grinding forces in UVG process is crucial both for a better understanding of the material removal mechanism in UVG, and for exploring the effective processing method to reduce the manufacturing defects[9].

Several significant investigations had been conducted based on the prediction of material removal rate in rotary ultrasonic machining by Pei et al. [10]. Following that, Liu et al. [11] proposed a mathematical model under the hypothesis that brittle fracture was the primary mechanism of material removal in ultrasonic machining for brittle materials and the relationship between machining parameters and

grinding force was discussed. In addition, Xiao et al. [12] considered the critical cutting depth of ductile-to-brittle transition for brittle materials and the average cutting depth in ductile and brittle regions respectively to develop the grinding force models in UVG. Sun et al. [13] developed a grinding force prediction model for UVG of glass material, and the grinding force was separated into three primary force components in the model. Amin et al.[14] developed a generalized cutting force model for rotary ultrasonic face milling of CFRP composite,and found the higher fluctuation due to the properties of materials. Baraheni et al.[15] predicted cutting force in rotary ultrasonic end grinding of Si_3N_4 ceramics based on the input machining variables.

However, only the average cutting depth and average chip thickness were considered in most models, and the nonuniform distribution of abrasive grits on the wheel would lead to different contact situations between the cutting tips and workpiece. The influence of the actual protrusion heights of grains on the grinding force was usually ignored. Feng et al. [16] proposed three kinds of tool-workpiece separation criterion based on kinematic analysis, and firstly predicted the cutting forces in feed, cutting and axial directions during all types of vibration assisted milling. Setti et al.[17] introduced an approach to predict the active grit number by considering the grits stochastic distribution, and then established an undeformed chip thickness model in micro grinding process based on the analysis of grit kinematics to deal with the limitations of idealized wheel surface topography in previous studies. Similarly, Jamshidi et al.[18] investigated the grinding parameters and active grit number influences on the grinding process mechanisms. Moreover, Yang et al.[19] investigated the varied lubricating conditions effects on the minimum chip thickness and ductile/brittle transition chip thickness in single-grit grinding process, and the location of size effect were also provided by analyzing the specific energy and grinding force curve in the model. However, the influences of grit kinematics on the geometric elements with consideration of ultrasonic vibration have not been revealed yet. Therefore, a theoretical grinding force prediction model has been established in UVG for fused silica glass with the consideration of both the nonuniform distribution of wheel morphologies and energy perspective in this work. Meanwhile, the predicted model was verificated by grinding experiments.

2. Development of grinding force model

2.1 Measurement and modelling of grinding wheel surface morphology

As the nonuniform distribution of the protrusion height of individual grits on the wheel surface would exert a great influence on the cutting force in UVG process. Therefore, the measurement and modelling of grinding wheel surface morphology are conducted to obtain the data of the protrusion height of these grits in this work.

Table 1 Technical data of the grinding wheel used in modelling.

Abrasive	Diamond
Bond type	Metal-bond
Outer diameter D_o(mm)	2
Interior diameter D_i(mm)	1
Abrasive mesh size S_a(μm)	58
Abrasive concentration C_a	100
Volume concentration V_g	25%

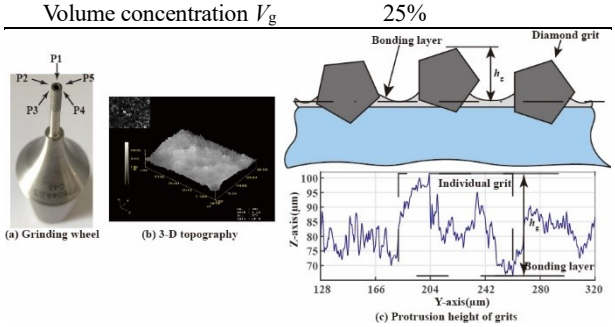

Fig. 1 Illustrations of measuring process for grinding wheel end-face topology.

As shown in Table 1 and Fig. 1(a), a diamond metal-bonded hollow grinding wheel was used in modelling of the wheel surface morphology. The wheel end-face was marked with 5 positions (P1-P5) for repeated measurements. A confocal laser scanning microscope (OLYMPUS OLS 3000) was employed to acquire the three-dimension topography of the grinding wheel surface, as shown in Fig. 1(b). The surface profile of the wheel surface is obtained by extracting the cross section in the axial direction. The individual grit with the bonding layer could be considered as a profile element. Then the height of these profile elements can be considered as the grain protrusion height hg, which is measured from the bonding layer (the lowest position in the profile element) to the grit top (exceeding the mesh size of grit) as shown in Fig. 1(c)[20]. At each marked sampling position, the axial ran-out of wheel is considered constant for all scanning grains.

The protrusion height of grits could be assumed to follow the normal distribution law[20, 21]. Fig. 2(a) presents the distribution frequency of the grit protrusion height h_g at marked positions. Obviously, the distribution of h_g at each position on the wheel surface approach to the normal distribution law. Therefore, the frequency histogram for h_g at all sampling positions is presented in Fig. 2(b).

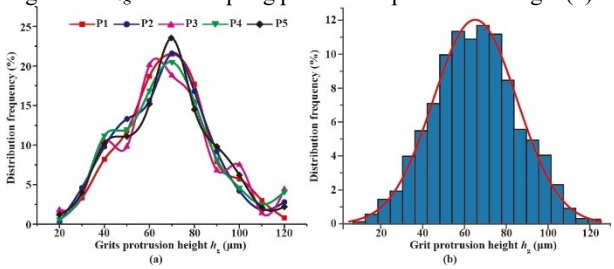

Fig. 2. Normal distribution plots of protrusion height of abrasive grain hg. (a) At each marked position, (b) At total five positions.

To verify the assumption, the methods of Kolmogorov-Smirnov test (K-S test) is performed to evaluate the normality degree of the grits protrusion height[22]. Indeed, the results (listed in Table 2) show that the significance value of K-S test is much larger than 0.05, which suggests that the data of h_g is in normal distribution. The statistical data of h_g are listed in Table 2.

Table 2 Kolmogorov-Smirnov test results and statistical data.

Sample size N	Mean value h_{meam} (μm)	Standard deviation value (μm)	Sig.
512×512	64.20	20.36	0.194

Since the measured data of h_g coincides with normal distribution

law, the modeled surface topology of the grinding wheel surface can be reconstructed by a $m\times n$ matrix, as expressed in Eq. (1)

$$\boldsymbol{H}=\left(h_{g,(i,j)}\right)_{m\times n} \tag{1}$$

where $h_{g,(i,j)}$ stands for h_g in the ith row and the jth column.

2.2 Kinematical analysis of the single diamond grit in UVG

The UVG process can be considered as the combination of the grinding and axial ultrasonic vibration of all grits on the grinding wheel. The motion of the single grit on the wheel consists of spindle rotation, horizontal feed motion and axial ultrasonic vibration in the coordinate system $Oxyz$. The initial phase of the ultrasonic vibration is assumed 0 at the beginning of grinding process. Therefore, the trajectory equation of the single grit in UVG can be expressed as Eq. (2):

$$S(t)=\begin{cases}S_x(t)\\S_y(t)\\S_z(t)\end{cases}=\begin{cases}0.5D_o\cos\omega t+v_f t\\0.5D_o\sin\omega t\\A\sin 2\pi ft\end{cases} \tag{2}$$

where D_o is the outer diameter of the grinding wheel, mm; $\omega=\pi n/30$ is the angular velocity of the grits, rad/s, n is the spindle rotation speed, rpm; v_f is the feed rate, mm/s; t is the cutting time, s; A is the ultrasonic vibration amplitude, μm; f is the vibration frequency, Hz. Moreover, the velocity of the single diamond grit ($v(t)$) in the coordinate system can be obtained by differentiating the Eq. (2).

2.3 Material removal rate modelling in UVG

The grinding experimental results present that the axial grinding force F_c is the main component among of three measured components of grinding force. Moreover, the impact-separation effect from ultrasonic vibration is mainly reflected in the axial direction.

During each ultrasonic vibration period, the grits are in noncontinuous contact with the workpiece surface for a certain period of time, as shown in Fig. 3. In the effective material removal process, the effective cutting time is Δt, and the maximum penetration depth is δ_m, From the kinematic trajectory equation of the single grit (Eq. (2)), the effective cutting time Δt can be expressed as:

$$\Delta t=2(t_2-t_1)=\frac{1}{\pi f}\left[\frac{\pi}{2}-\arcsin\left(1-\frac{\delta_m}{A}\right)\right]\approx\frac{\delta_m}{2Af} \tag{3}$$

where, δ_m is the maximum penetration depth between the grits and workpiece surface, mm.

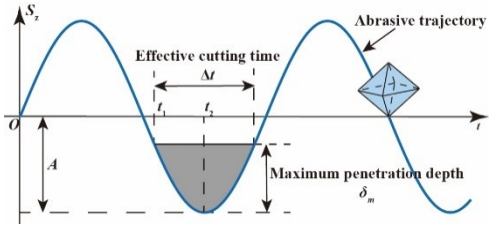

Fig. 3. Schematic illustration of effective cutting time in a single vibration period.

Then the effective cutting length of single grit l_s in the effective cutting time Δt can be determined by the velocity of the abrasive grit $v(t)$ and the effective cutting time Δt:

$$l_s=\int_{t_1}^{t_2}v(t)dt\approx\frac{\pi n(D_o+D_i)}{120}\Delta t \tag{4}$$

In UVG process of fused silica glass, as shown in Fig. 4(a), the grit penetration depth increases from δ=0 to $\delta=\delta_m$ and then declines to δ=0 during a single effective cutting time, as the grit goes through the effective cutting length l_s on the workpiece. In Fig. 4(b), half of the brittle fracture region is simplified as a tetrahedron HABC, in which the straight-line HC and HB represent the lateral cracks induced as the penetration depth reaching δ_m. Therefore, the theoretical material removal volume V can be expressed as: $V=2V_{HABC}=C_LC_hl_s/3$. The lateral crack characteristic dimension of the length C_L and the depth C_h can be calculated by[23]:

$$\begin{cases}C_L=C_2\tan^{-5/12}\theta\left[\dfrac{E^{3/4}}{H_vK_{IC}\left(1-\upsilon^2\right)^{1/2}}\right]^{1/2}F_m^{5/8}\\C_h=C_2\tan^{-1/3}\theta\dfrac{E^{1/2}}{H_v}F_m^{1/2}\end{cases} \tag{5}$$

where C_2 is a dimensionless constant depending on the indenter system, and C_2=0.226; θ is the semi-angle between two opposite edge of the grits; K_{IC} is the fracture toughness of workpiece materials; H_v is the Vickers hardness; υ is the Poisson's ratio; E is the elastic modulus; and F_m is the maximum contact force for the single grit, N.

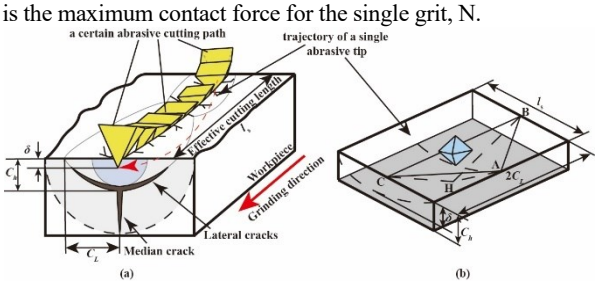

Fig. 4. Schematic illustration of material removal process in brittle fracture mode in UVG. (a) Microscopic view of grinding process, (b) The volume of brittle fracture material removal by single grit.

Thus, the theoretical material removal rate for single grit M_T is defined as:

$$M_T=Vf=C_LC_hl_sf/3 \tag{6}$$

And the material removal rate for all the effective grits M can be obtained by the effective grits number N_e and theoretical material removal rate M_T:

$$M=N_eM_T=C_0\frac{C_a^{2/3}A_0}{3S_a^2}C_LC_hl_sf \tag{7}$$

where C_0 is a dimensionless constant related to the density of abrasive material, for diamond, C_0=0.03; C_a is the grit concentration, and S_a is the grit size; A_0 is the contact area of the grinding wheel surface. Additionally, the mean values of abrasive size (S_a), is approximate to the mean values of the protrusion height of abrasive grits, (h_{mean}).

Meanwhile, the actual material removal rate M_a can be presented as: $M_a=A_0\cdot v_f$. Then the correction coefficient K will be introduced to correct the different between M_a and M, which could be presented as:

$$M_a=K\cdot M \tag{8}$$

where K is a proportionality coefficient, and it is assumed to be constant for a certain workpiece-tool system.

2.4 Gringding force prediction model in UVG

Since the ultrasonic vibration superposes along the axial direction, only the effect of impact force is taken account in the grinding force model. For the effective grits the maximum impact force F_n could be derived by F_m[24]:

$$F_n = N_e \cdot F_m = N_e \zeta \delta_m^2 \tan\theta H_\upsilon / 2 \tag{9}$$

The grits could be regarded as an ideal rigid body with incompressibility and the effective cutting time Δt is very short from Eq. (3) ($\delta_m << Af$), the impulse I in term of the impact force over the time $F(t)$ during one ultrasonic vibration period can be approximated to the impulse in term of the maximum impact force F_m. Thus, the impulse I can be described as:

$$I = \int_T F(t)dt \approx F_n \Delta t \tag{10}$$

The impulse I also can be expressed in term of the grinding force F_c during one ultrasonic vibration period: $I=F_c/f$.

Due to these impulse values I are actually on behalf of the same physical process, so there is:

$$F_c = F_n \cdot \Delta t \cdot f = N_e F_m \Delta t f \tag{11}$$

By substituting Eq. (3), (4), (5), and (7) into Eq. (8), the maximum penetration depth δ_m can be expressed as:

$$\delta_m = \left[\frac{C_3}{K} \cdot \frac{v_f A K_{IC}^{1/2} \left(1-\upsilon^2\right)^{1/4} H_\upsilon^{3/8} \cot^{3/8}\theta}{n C_a^{2/3} R E^{7/8} \zeta^{9/8}} h_{mean}^2 \right]^{4/13} \tag{12}$$

where $C_3 = 180 \cdot \left(C_0 C_2^2 \pi\right)^{-1}$.

According to the section 2.1, the protrusion height of the grits h_g follows the normal distribution. Therefore, the maximum penetration depth δ_m also follows normal distribution law. By substituting the reconstruction wheel surface model from Eq. (1) into Eq. (12), and rewritten Eq. (11), the grinding force F_c could be presented as:

$$F_c = \sum_{i,j=1}^{N_e} f \cdot F_m^{(i,j)} \left(\delta_{m,(i,j)} \right) \Delta t \tag{13}$$

3. Verification of the proposed grinding force model

In order to validate the grinding force prediction model developed in this study, the validation experiments with varied grinding and ultrasonic parameters are performed.

The axial ultrasonic vibration grinding experiments were conducted on a five-axis precision ultrasonic machine center (DMG Ultrasonic 70-5 Linear). Fig. 5 shows the entire grinding experiment setup. The grinding tool is fixed on the ultrasonic spindle system and oscillates along the axial direction of the spindle with the resonance frequency of machine system at 30kHz and the maximum amplitude is 10μm for the selected grinding tool.

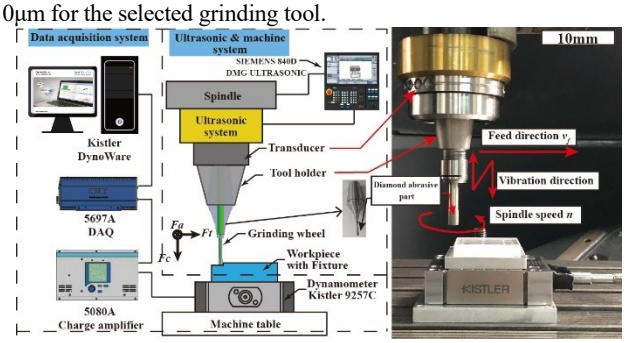

Fig. 5. Schematic of the UVG experiment setup

The diamond metal-bonded tools are provided by SCHOTT Diamond Tools Corp. (Stadtoldendorf, Germany). The detailed technical data of the diamond tools used in the experiments are listed in Table 1. The fused silica glass specimen with the dimension of 30mm (length)×30mm (width)×8mm (height) was used in the experiments, the material properties are shown in Table 3. To reduce influences from previous defects and scratches, the polishing operation was conducted on the specimen surface before experiments.

Table 3 Material properties of fused silica glass.

Property	Unit	Value
Density ρ	g/cm^3	2.530
Elastic modulus E	GPa	82
Poisson's ratio υ	-	0.28
Fracture toughness K_{IC}	MPa·m$^{1/2}$	0.82
Vickers hardness H_v	GPa	7.2

The grinding parameters of verification experiments are given in the Table 4. The grinding force were measured by a Kistler 9257C dynamometer, whose sampling frequency was 10kHz, as shown in Fig. 5.

Table 4 Experiments design for verifying the prediction model.

Spindle speed n (rpm)	Feed rate v_f (mm/min)	Cutting depth a_p (μm)	Amplitude A (μm)
6000,8000,10000, 12000,14000	60	20	10
10000	40,50,60,70,80	20	10
10000	60	10,15,20,25,30	10
10000	60	20	0,2,4,6,8,10

The comparison between average experimental and predicted cutting force results has been shown in Fig. 6. It can be seen from Fig. 6(d) that the average grinding force is 15.45N for conventional grinding (A=0). As the vibration amplitude is 2μm, the average grinding force is 12.12N for UVG. The average grinding forces decrease by 21.6% when the ultrasonic vibration is exerted on the grinding tool and the average grinding forces keep declining trend when vibration amplitude increases.

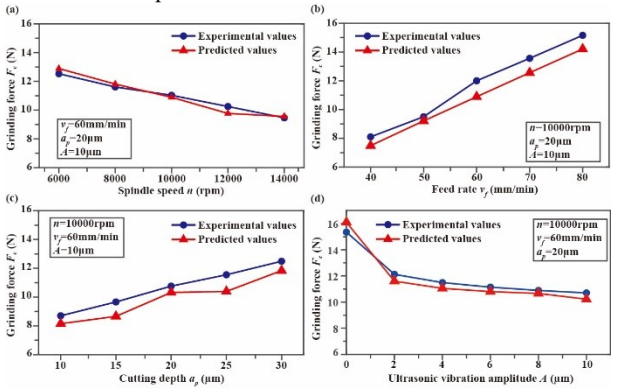

Fig. 6. Experimental and predicted average grinding force values comparison

It is found that the corresponding prediction values for the cutting force are consistent with the experimental results in given parameters ranges. Meanwhile, the average values of relative error for each varied parameter have been listed in Table 6. The maximum average relative error between predicted and experimental results is 10.37%, and the total relative average error is 4.94%. The proposed model in this work shows approximate or better predicted ability comparing with some existing models.

To provide a comprehensive comparison between the proposed model and previous cutting force models, a list of relative error of these prediction models with similar conditions is presented in Table 5, and the proposed model shows approximate or better predicted ability comparing with these existing models.

Table 5 Comparison of relative error of cutting force between experim ental and prediction results.

	Machining type	Material	Relative error
Current model	AUVEG	BK7 optical glass	4.94% of mean error
Bertsche et al.[25]	Rotary ultrasonic face milling	Ceramic matrix composite	Qualitative comparison
Zhang et al.[26]	Rotary ultrasonic face milling	K9 optical glass	Qualitative comparison
Xiao et al.[12]	AUVSG	Zirconia ceramics	14.40% of mean error
Sun et al.[27]	AUVSG	Zerodur	7.37% in normal direction and 11.53% in tangential direction
Yang et al.[28]	AUVEG	ZrO_2 ceramic	12% of mean error
Baraheni et al.[15]	AUVEG	Si_3N_4	17.27% of mean error

4. Conclusion

In this paper, a theoretical model was proposed for predicting grinding force in axial ultrasonic vibration grinding of fused silica glass. As an innovation, this prediction model introduced a novel method to consider the effect of nonuniform distribution of protrusion height of grits on the grinding force. The validation experiments were conducted to demonstrate the effectiveness of this prediction model, and the predicted values of cutting force were found to agree well with the experimental results and the average relevant error is 4.94%.

ACKNOWLEDGEMENT

REFERENCES

1. Moore, L. A. and Smith, C. M., "Fused Silica as an Optical Material [Invited]," Opt. Mater. Express, Vol. 12, No. 8, pp. 3043-3059, 2022.
2. Wei, W., Yao, P., Wang, J. et al., "Elastic Stress Field Model and Micro-Crack Evolution for Isotropic Brittle Materials During Single Grit Scratching," Ceram. Int., Vol. 43, pp. 10726-10736, 2017.
3. Goel, S., Luo, X., Agrawal, A. et al., "Diamond Machining of Silicon: A Review of Advances in Molecular Dynamics Simulation," Int. J. Mach. Tools Manuf., Vol. 88, pp. 131-164, 2015.
4. Yang, Z., Zhu, L., Zhang, G. et al., "Review of Ultrasonic Vibration-Assisted Machining in Advanced Materials," Int. J. Mach. Tools Manuf., Vol. 156, p. 103594, 2020.
5. Pei, Z. J., Ferreira, P. M., Kapoor, S. G. et al., "Rotary Ultrasonic Machining for Face Milling of Ceramics," Int. J. Mach. Tools Manuf., Vol. 35, No. 7, pp. 1033-1046, 1995.
6. Singh, R. P. and Singhal, S., "Rotary Ultrasonic Machining: A Review," Mater. Manuf. Process., Vol. 31, No. 14, pp. 1795-1824, 2016.
7. Pereverzev, P. P. and Pimenov, D. Y., "A Grinding Force Model Allowing for Dulling of Abrasive Wheel Cutting Grains in Plunge Cylindrical Grinding," J. Frict. Wear., Vol. 37, No. 1, pp. 60-65, 2016.
8. Zhang, J., Li, H., Zhang, M. et al., "Study on Force Modeling Considering Size Effect in Ultrasonic-Assisted Micro-End Grinding of Silica Glass and Al_2O_3 Ceramic," Int. J. Adv. Manuf. Technol., Vol. 89, No. 1-4, pp. 1173-1192, 2017.
9. Baraheni, M. and Amini, S., "Predicting Subsurface Damage in Silicon Nitride Ceramics Subjected to Rotary Ultrasonic Assisted Face Grinding," Ceram. Int., Vol. 45, No. 8, pp. 10086-10096, 2019.
10. Pei, Z. J., Prabhakar, D., Ferreira, P. M. et al., "A Mechanistic Approach to the Prediction of Material Removal Rates in Rotary Ultrasonic Machining," J. Manuf. Sci. Eng., Vol. 117, No. 2, pp. 142-151, 1995.
11. Liu, D., Cong, W. L., Pei, Z. J. et al., "A Cutting Force Model for Rotary Ultrasonic Machining of Brittle Materials," Int. J. Mach. Tools Manuf., Vol. 52, No. 1, pp. 77-84, 2012.
12. Xiao, X., Zheng, K., Liao, W. et al., "Study on Cutting Force Model in Ultrasonic Vibration Assisted Side Grinding of Zirconia Ceramics," Int. J. Mach. Tools Manuf., Vol. 104, pp. 58-67, 2016.
13. Sun, G. Y., Zhao, L. L., Zhao, Q. L. et al., "Improved Force Prediction Model for Grinding Zerodur Based on the Comprehensive Material Removal Mechanism," Appl. Opt., Vol. 57, No. 14, pp. 3704-3713, 2018.
14. Amin, M., Yuan, S., Khan, M. Z. et al., "Development of a Generalized Cutting Force Prediction Model for Carbon Fiber Reinforced Polymers Based on Rotary Ultrasonic Face Milling," Int. J. Adv. Manuf. Technol., Vol. 93, No. 5-8, pp. 2655-2666, 2017.
15. Baraheni, M. and Amini, S., "Mathematical Model to Predict Cutting Force in Rotary Ultrasonic Assisted End Grinding of Si_3N_4 Considering Both Ductile and Brittle Deformation," Measurement, Vol. 156, p. 107586, 2020.
16. Feng, Y., Hsu, F.-C., Lu, Y.-T. et al., "Force Prediction in Ultrasonic Vibration-Assisted Milling," Mach. Sci. Technol., Vol. 25, No. 2, pp. 307-330, 2020.
17. Setti, D., Arrabiyeh, P. A., Kirsch, B. et al., "Analytical and Experimental Investigations on the Mechanisms of Surface Generation in Micro Grinding," Int. J. Mach. Tools Manuf., Vol. 149, p. 103489, 2020.
18. Jamshidi, H., Gurtan, M., and Budak, E., "Identification of Active Number of Grits and Its Effects on Mechanics and Dynamics of Abrasive Processes," J. Mater. Process. Technol., Vol. 273, p. 116239, 2019.
19. Yang, M., Li, C., Zhang, Y. et al., "Effect of Friction Coefficient on Chip Thickness Models in Ductile-Regime Grinding of Zirconia

Ceramics," Int. J. Adv. Manuf. Technol., Vol. 102, No. 5-8, pp. 2617-2632, 2019.
20. Dai, C. W., Yin, Z., Ding, W. F. et al., "Grinding Force and Energy Modeling of Textured Monolayer CBN Wheels Considering Undeformed Chip Thickness Nonuniformity," Int. J. Mech. Sci., Vol. 157, pp. 221-230, 2019.
21. Zhou, X. and Xi, F., "Modeling and Predicting Surface Roughness of the Grinding Process," Int. J. Mach. Tools Manuf., Vol. 42, pp. 969-977, 2002.
22. Ding, W. F., Dai, C. W., Yu, T. Y. et al., "Grinding Performance of Textured Monolayer CBN Wheels: Undeformed Chip Thickness Nonuniformity Modeling and Ground Surface Topography Prediction," Int. J. Mach. Tools Manuf., Vol. 122, pp. 52-66, 2017.
23. Lawn, B. R., Evans, A. G., and Marshall, D. B., "Elastic/Plastic Indentation Damage in Ceramics: The Median/Radial Crack System," Journal of the American Ceramic Society, Vol. 65, No. 11, pp. 561-566, 1982.
24. Wang, J., Feng, P., Zhang, J. et al., "Investigations on the Critical Feed Rate Guaranteeing the Effectiveness of Rotary Ultrasonic Machining," Ultrasonics, Vol. 74, pp. 81-88, 2017.
25. Bertsche, E., Ehmann, K., and Malukhin, K., "An Analytical Model of Rotary Ultrasonic Milling," Int. J. Adv. Manuf. Technol., Vol. 65, No. 9-12, pp. 1705-1720, 2013.
26. Zhang, C., Zhang, J., and Feng, P., "Mathematical Model for Cutting Force in Rotary Ultrasonic Face Milling of Brittle Materials," Int. J. Adv. Manuf. Technol., Vol. 69, pp. 161-170, 2013.
27. Sun, G., Zhao, L., Ma, Z. et al., "Force Prediction Model Considering Material Removal Mechanism for Axial Ultrasonic Vibration-Assisted Peripheral Grinding of Zerodur," Int. J. Adv. Manuf. Technol., Vol. 98, No. 9-12, pp. 2775-2789, 2018.
28. Yang, Z., Zhu, L., Lin, B. et al., "The Grinding Force Modeling and Experimental Study of Zro_2 Ceramic Materials in Ultrasonic Vibration Assisted Grinding," Ceram. Int., Vol. 45, No. 7, pp. 8873-8889, 2019.